RSC Advances

ROYAL SOCIETY OF CHEMISTRY

www.rsc.org/advances

Edge functionalized graphite (EF-graphite) nanoplatelates were prepared by L-phenylalanine through Friedel-Crafts acylation reaction. The resultant EF-graphite are highly dispersible in various polar solvents and shows enhanced electron transfer capability compared to pristine graphite.

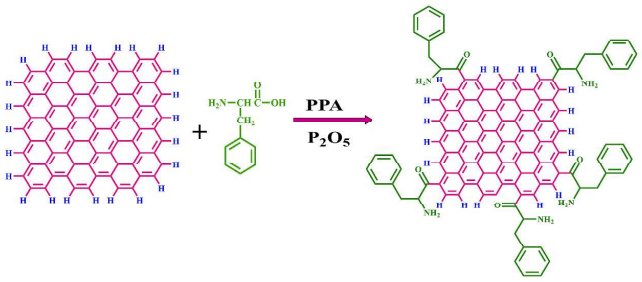

Cite this: DOI: 10.1039/c0xx00000x

www.rsc.org/xxxxxx

ARTICLE TYPE

Structure, morphology and electronic properties of L-phenylalanine edge-functionalized graphite platelets through Friedel-Crafts acylation reaction

Amir Abdolmaleki,*[a,b,c] Shadpour Mallakpour*[a,b,c] and Sedigheh Borandeh[a]

Received (in XXX, XXX) Xth XXXXXXXXX 20XX, Accepted Xth XXXXXXXXX 20XX
DOI: 10.1039/b000000x

In this study, in order to develop functionalized graphite without damaging the graphitic basal plane, graphite was edge-selectively functionalized with biosafe L-phenylalanine amino acid through direct Friedel-Crafts acylation reaction in polyphosphoric acid/phosphorus pentoxide medium. This technique led to graft amino acid moieties to the defective sites (mostly sp^2 C–H) located mainly on the edges of graphite via electrophilic substitution reaction. The presence of L-phenylalanine attached onto the graphite edge was confirmed by using elemental analysis, X-ray photoelectron spectroscopy (XPS) and thermal gravimetric analysis. In addition, the covalent functionalization was confirmed by Fourier transform infrared spectroscopy, XPS, and Raman spectroscopy. Additionally, cyclic voltammetry was used to investigate the electrochemical behavior of edge functionalized graphite.

Introduction

During the past few years, nano-science and nanotechnology development have been marked by a strong increase in attention to different nanomaterials especially to graphene-based ones owing to its promising properties, such as excellent mechanical strength, high thermal conductivity, large specific surface area, and ultrahigh electron-transport properties.[1-5] Graphene, the thinnest known material, is a two dimensional hexagonal structure consisting of sp^2-hybridized carbon atoms arranged in a honeycomb structure. It has inspired enormous potential applications in various electronic devices such as touch panels, p–n junction materials, flexible thin-film transistors, and solar cells owing to its unusual electronic structure.[6-9]

Although graphene has the potential to maintain the outstanding properties in order to be utilized in several areas, it is extremely complicated to attain a suitable solvent for dispersing the highly stacked graphite sheets, which are caused by its great π-π stacking and lower functionality. In order to overcome this limitation, functionalization of graphene sheets through covalent or non-covalent interactions has been explored to improve its dispersibility in various media.[10-15] One of the most widespread ways to functionalize graphene platelets is the modification of graphene oxide (GO) using numerous organic molecules, bio-molecules and polymers.[12, 15-18] GO comprises a wide range of oxygen functional groups such as epoxide and hydroxy groups on the basal planes, and carboxyl and ketone groups at the edges.[19-22] However, this way of modification is problematic because of tending to reduce the electrical conductivity of graphene owing to its intrinsic insulating effect, which limits the convenient applicability of the functionalized graphene in nano-electronic fields.[23] In this way of functionalization, the sp^2-hybridized carbon in graphene converts into tetrahedral sp^3-hybridized carbon, which causes a loss of the free, sp^2-associated π electron constituting the π-cloud on graphene. The removal of the π electron from the carbon atom reduces the carrier density and can introduce a band gap (via removal of electronic states) and/or a transport barrier. Therefore, a combination of the carrier deficiency at the sp^3 site, the associated disruption of the electron-potential continuum, and the distorted planar lattice causes a drastic reduction in graphene's carrier mobility and a change in charge polarity/density.[23]

To recover the graphene conjugated structure and to reproduce electrically conducting graphene platelets, surface modification of GO followed by reduction has been reported. The most straightforward aim of functionalized GO reduction is to fabricate graphene-like materials similar to pristine graphene obtained from exfoliation of individual layers of graphite in structure and properties. Though the obtained reduced functionalized GO is more defective and thus less conductive than pristine graphene,[24-29] residual functional groups and chemical or structural defects significantly alter the structure of graphene basal plane. Therefore, it is not appropriate to refer to reduced GO since the properties are extensively different.

Recently, graphite nanosheets were covalently functionalized without the basal plane oxidation or any damage on the basal plane surface of graphite through electrophilic substitution of sp^2 C–H, which is located mainly on the edges of graphite. The edge-functionalized graphite (EF-graphite) is highly dispersible in various polar solvents to self-exfoliate into graphene nanosheets, thus becoming suitable for simple solution processing. Compared to GO, the edge-selective functionalization of graphite could maintain the high crystalline graphitic structure on its basal plane.

The edge-attached functional groups lead to enhance the dispersion of graphene in solvents to improve graphene processability.[30-35] Moreover, EF-graphite demonstrates promising potential applications in various fields, such as highly conductive large-area films, metal-free electrocatalysts for the oxygen-reduction reaction (ORR), and as additives in composite materials with enhanced properties.[32-34, 36-38]

In this study, a reaction was established to selectively attach the eco-friendly and biocompatible L-phenylalanine on the edge of graphite using a direct Friedel-Crafts acylation in a polyphosphoric acid (PPA)/ phosphorus pentoxide (P_2O_5) medium. The structure and morphology of solid EF-graphite were investigated. Moreover, the thermal and electrical properties of resulted EF-graphite were studied.

Experimental

Materials

Natural graphite powder (diameter 5–10 μm, thickness 4-20 nm, layers < 30 and purity >99.5 wt%), was purchased from Neutrino Co. (Iran). Other chemicals used in this study were obtained from Fluka Chemical Co. (Switzerland) and Merck Chemical Co. (Germany) and were used without further purification.

Instrumentation

FT-IR spectra of the samples were recorded on a Jasco-680 (Japan) spectrometer using KBr pellets. Elemental analysis was performed with a CHNS-932, Leco. XRD was used to characterize the crystalline structure of the materials. XRD patterns were collected using a Bruker, D8 Advanced diffractometer with a copper target at the wave length of λ CuK_α = 1.5406 Å and a tube voltage of 40 kV and tube current of 35 mA, in the range of 5–100° at the speed of 0.05 °/min. Raman spectroscopy was recorded from 500 to 3500 cm^{-1} on a Almega Thermo Nicolet Dispersive Raman Spectrometer using a Nd:YLF laser source operating at wavelength of 532 nm. X-ray photoelectron spectroscopy (XPS) was utilized to investigate chemical states variations of the EF-graphite using twin anode XR3E2 X-ray Al based source system operating at a vacuum by X-ray 8025-BesTec spectrometer. The XPS data were analyzed by Casa XPS software. Thermogravimetric analysis (TGA) is performed with a STA503 win TA (Bahr-Thermoanalyse GmbH, Hüllhorst, Germany) at the heating rate of 10°C/min from 25 to 800 °C under nitrogen atmosphere. The morphology of EF-graphite was observed using FE-SEM (HITACHI S-4160, Japan). TEM image was obtained using Philips CM 120 operated (Netherlands) at voltage of 150 kV. Electrochemical measurements were performed using a potentiostat–galvanostat AutoLab with a conventional three-electrode system. The system was run on a PC using GPES and FRA 4.9 software. Potentials were measured versus a saturated Ag/AgCl (3 M NaCl) electrode. Also, samples/glassy carbon (GC) electrode were used as the working electrode, a platinum wire as the counter electrode, and an Ag/AgCl (3 M NaCl filled) electrode as the reference electrode for measuring cyclic voltammetry (CV).

Edge-functionalization of graphite using L-phenylalanine

L-phenylalanine (0.15 g, 0.9 mmol), graphite (0.1 g), PPA (83% P_2O_5 assay: 5 g), and P_2O_5 (1 g) were placed and mechanically stirred at 130 °C for 72 h. The initially black mixture became lighter and viscous as the functionalization onto graphite progressed. At the end of the reaction, water was added into the flask. The obtained precipitate was collected by centrifuge at 3000 rpm, Soxhlet-extracted with water, and then with methanol overnight. Ultimately, the EF-graphite was dried at 80 °C under reduced pressure.

Electrochemical Study

CV was used to examine the electrochemical behavior of EF-graphite and comparing with natural graphite electrical properties. For CV measurements, an aqueous solution of NaOH (0.1 M) was used as the electrolyte. N_2 was used to purge the solution to achieve oxygenfree electrolyte solution. The procedures of GC electrode pretreatment and modification are described as follows: prior to use, the working electrode was polished with alumina slurry to obtain a mirror-like surface and then washed with deionized (DI) water and allowed to dry. The EF-graphite (1 mg) was dissolved in 1 mL DI water by sonication. The EF-graphite suspension (5 μL) was pipetted on the glassy carbon (GC) electrode surface, followed by drying at room temperature.

Results and discussion

Graphite was edge-selectively functionalized with L-phenylalanine, a biocompatible and environmentally friendly molecule, in polyphosphoric acid (PPA)/phosphorus pentoxide (P_2O_5) medium (Fig. 1). Generally, the interior basal plane surfaces of graphite are stacked due to strong π–π interactions, and only the edges of graphite are more available. Therefore, the sp^2 C–H groups at the edges of graphite are the best sites where the electrophilic substitution reactions can happen. In the reaction medium, PPA, a viscous mild polymeric acid ($pK_a \approx 2.1$) which plays two essential roles for dispersion and functionalization of graphite,[30] was used. The most crucial features of the employed reaction condition in this study are that the PPA/P_2O_5 medium leads to selective functionalization at the edges of graphite without any oxidation occurring on graphite sheets.[31, 32]

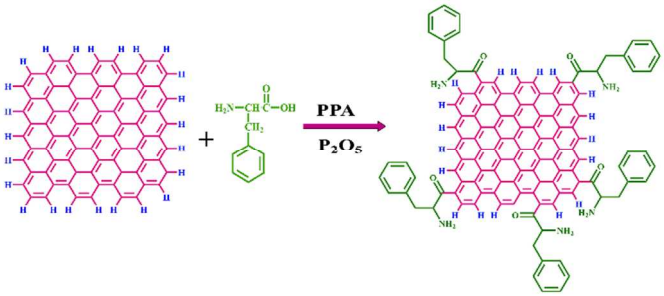

Fig. 1 Preparation of EF-graphite with L-phenylalanine through direct Friedel-Crafts acylation reaction in PPA/P_2O_5 medium.

Elemental analysis was used to confirm and determine the degree of graphite functionalization. The elemental analysis data presented in Table 1 revealed that the pristine graphite contained a considerable amount of sp^2 hydrogen (0.65 wt.%) at its edges. In addition, based on pristine graphite elemental analysis data, some amount of oxygen located on the graphite surface was seen. Moreover, to examine the effect of PPA/P_2O_5 media on the

graphite structure and to refuse oxidation of graphite in PPA/P_2O_5 condition, graphite was treated by PPA/P_2O_5 without L-phenylalanine. The obtained elemental analysis data for PPA/P_2O_5 treated graphite is approximately similar to pristine graphite and only a little changes were observed compared to pure graphite. Consequently, it seems that unlike strong acid treatment such as HNO_3/H_2SO_4, PPA/P_2O_5 treatment causes very slight oxidation of graphite. By comparing the elemental concentration of carbon, hydrogen and nitrogen before and after functionalization, the production of EF-graphite was confirmed.

Table 1 Elemental analysis of pristine graphite and EF-graphite.

Sample	C (wt.%)	N (wt.%)	H (wt.%)	O (wt.%)
Pristine graphite	96.32	0.00	0.65	3.03
PPA/P_2O_5 treated Graphite	94.38	0.00	0.89	4.73
EF-graphite	79.21	1.87	1.14	17.78

The amount of L-phenylalanine grafted onto the edge of graphite was calculated through the following equation,[39] using EF-graphite nitrogen content.

$$\frac{\text{mol}}{\text{g}} = \frac{\left(\frac{W_t \times 100}{X}\right) \times \frac{100}{100-\left(\frac{W_t \times 100}{X}\right)}}{Y}$$

Where, W_t is the weight percent of the element measured, X is the theoretical weight percent of the element in the molecule and Y is the theoretical M_w of the molecule. L-Phenylalanine has carbon, hydrogen and nitrogen contents of 65.44, 6.71 and 8.48 wt.% with a M_w of 165.19 g/mol. Based on this equation, the amount of L-phenylalanine detected from nitrogen contents is 0.17 mol/g.

In order to identify the functional groups changes before and after functionalization of graphite, FT-IR has been performed. Fig. 2 displays the FT-IR spectra of pristine graphite, EF-graphite, PPA/P_2O_5 treated graphite, graphite + L-phenylalanine and L-phenylalanine. The pristine graphite demonstrates a featureless spectrum except for a peak at 1570 cm^{-1}, which corresponds to the C=C bonds of graphite. EF-graphite exhibits several characteristic peaks. The peak at 3438 cm^{-1} is attributed to the $-NH_2$ groups of amino acid and the one at 2923 cm^{-1} corresponds to the aliphatic sp^3 C-H stretching. Furthermore, EF-graphite displays a strong carbonyl (C=O) stretching peak at 1721 cm^{-1}, which provides further evidence indicating that the L-phenylalanine moieties were covalently linked to the graphite. For more comparison, the FT-IR spectrum of L-phenylalanine was also shown in Fig. 2. L-Phenylalanine FT-IR spectrum doesn't show any peak at 1720 cm^{-1}; so, it is concluded that L-phenylalanine moieties were covalently linked to the graphite. In addition, to confirm covalently functionalization of graphite, similar ratio of graphite and L-phenylalanine were completely ground and FT-IR was taken. As shown in Fig. 2, the FT-IR spectrum of graphite/phenylalanine shows no new peak compared to pure graphite and L-phenylalanine. So, the physically adsorbed L-phenylalanine onto graphite was denied.

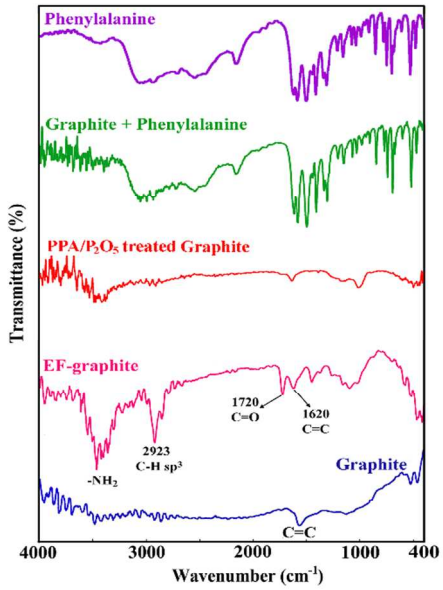

Fig. 2 FT-IR spectra of graphite, EF-graphite, PPA/P_2O_5 treated graphite, graphite + phenylalanine and phenylalanine.

TGA analysis was used to estimate the quantitative amount of graphite functionalization. TGA thermograms of graphite and EF-graphite are shown in Fig. 3. The pure graphite exhibited no weight loss up to a temperature of 800 °C while EF-graphite demonstrated a stepwise weight loss beginning at 350 °C. This weight loss can be attributed to the L-phenylalanine moieties that were covalently attached to the edges of graphite. The degree of covalently attached amino acid molecules was estimated from the weight loss differences between graphite and EF-graphite at 800 °C, which is approximately 20 wt.%. Furthermore, EF-graphite thermogram shows no weight loss around 100-200 °C, which is the characteristic of the bound water trapped in graphene oxide (GO). Therefore, it is concluded that the graphite is not oxidized during the edge-functionalization in PPA/P_2O_5 medium.

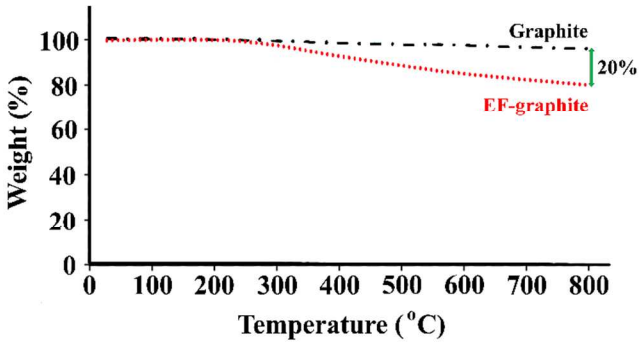

Fig. 3 TGA thermograms of graphite and EF-graphite using a heating rate of 10 °C min^{-1} in nitrogen.

The XRD patterns of graphite and EF-graphite are presented in Fig. 4. A sharp diffraction peak at $2\theta = 26.6^\circ$ is observed in the XRD diffraction pattern of graphite, which is assigned to the (002) crystal planes of graphite with an interlayer d-spacing of 3.26 Å. The same peak located at $2\theta = 26.5^\circ$ is observed in the XRD pattern of EF-graphite and reveals that L-phenylalanine moieties were completely attached to the edges of graphite without any functionalization occurring on the basal plane.

Unlike GO, which has a significant shift of the (002) peak to the lower area (2θ = 11.6° and d-spacing of 7.7 Å),[40, 41] in EF-graphite, the (002) peak remains at the same location with weaker intensity. In addition, a low intensity broad peak centered at 2θ = 20° is observed, which can be due to the presence of amino acid molecules. These results revealed that the edges of EF-graphite are delaminated without any more lattice expansion.

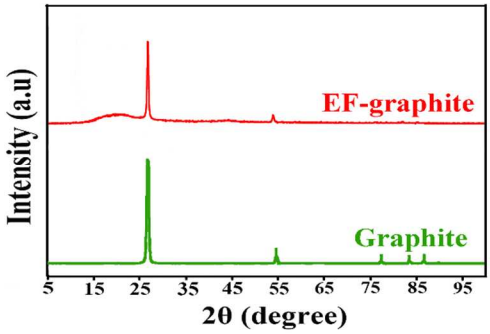

Fig. 4 The XRD patterns of graphite and EF-graphite.

Raman spectroscopy was performed to characterize the quality of pure graphite and EF-graphite and is shown in Fig. 5. In general, the Raman spectrum of pure graphite consists of an important peak at 1566 cm^{-1} (G band), which is attributed to the first order scattering of the E_{2g} phonon from sp^2 carbon atoms with a small D band at around 1332 cm^{-1} associated with the edge distortions and topological defects. In contrast, the EF-graphite displays the G band at 1584 cm^{-1} and a strong D band around 1341 cm^{-1} with the I_D/I_G ratio of 0.6. The presence of D band can be due to edge distortion or defects by functionalization. In addition, EF-graphite exhibits a new peak at 1620 cm^{-1} (D′ band) at the right shoulder of the G bands. This stems from another weak disorder on the graphitic structure owing to edge functionalization. A peak at 1421 cm^{-1} corresponds to C-H bond inserted at the edge of graphite.[33, 42]

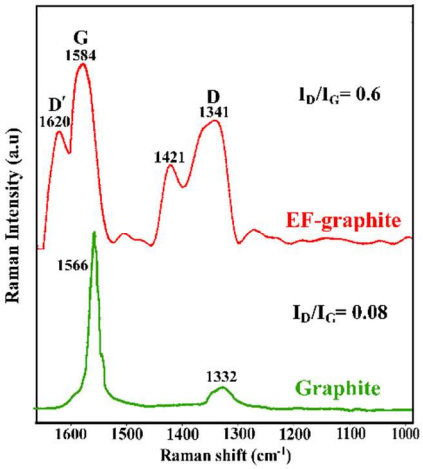

Fig. 5 Raman spectra of graphite and EF-graphite.

Further evidence for graphite functionalization was obtained through XPS spectroscopic measurements as shown in Fig. 6. The survey XPS spectrum of EF-graphite exhibits three peaks centered at 284, 399 and 532 eV, which are assigned to C1s, N1s and O1s signals, respectively. The appearance of N1s and O1s in the XPS spectrum of EF-graphite confirms that amino acid moieties are successfully attached to the graphite platelets. Pristine graphite contains only a trace of O, which comes from the physically adsorbed oxygen; but after edge functionalization, the O1s peak intensity was significantly increased. The C/O ratio for EF-graphite is 2.4, which is higher than that of GO (C/O = 0.64). The C/O ratio clearly indicates that GO contains more oxygen-rich functional groups than the EF-graphite with its edge only being functionalized with L-phenylalanine in PPA/P_2O_5 medium. In addition, the elemental composition of the EF-graphite was further characterized using XPS. As summarized in Table 2, the elemental composition is presented in terms of atomic percent (at%) for XPS. The carbon content of EF-graphite was significantly less than that of pristine graphite (86.49%), implying that heteroatoms had been introduced at the edges of graphite. As shown in Table 2, XPS analysis data clearly exhibited the presence of nitrogen (1.23 at.%) after functionalization.

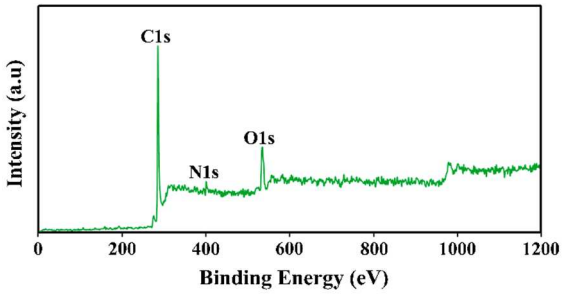

Fig. 6 The survey XPS spectrum of EF-graphite.

Table 2 XPS analysis data for EF-graphite.

Sample	Composition (at.%)		
	C	N	O
EF-graphite	86.49	1.23	12.28

FE-SEM was used to investigate the morphology of EF-graphite. Fig. 7 exhibits the FE-SEM images of EF-graphite in different magnification. The FE-SEM images show that the edges of EF-graphite are delaminated which can improve EF-graphite dispersion in polar solvents.

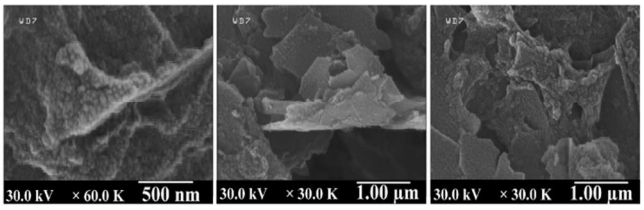

Fig. 7 FE-SEM images of EF-graphite in different magnification.

TEM provides direct observation for the morphology of EF-graphite. Fig. 8 displays TEM images of EF-graphite in different areas. EF-graphite exhibits edge wrinkled and sheet-like structures. The TEM images show that the basal plane surfaces of graphite have not been changed and/or damaged throughout the functionalization and workup processes.

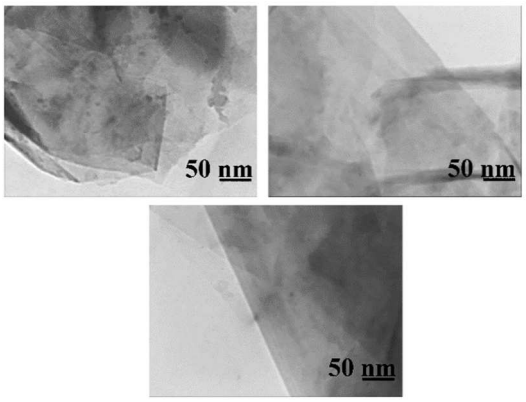

Fig. 8 TEM images of EF-graphite.

The electrochemical performances of EF-graphite were evaluated by CV, and were compared with pure graphite as shown in Fig. 9. The CV curves of graphite and EF-graphite demonstrated similar behavior and shape without obvious oxygen evolution peaks, indicating good charge propagation with electrodes. This denotes that by edge functionalization, the sp^2 hybridization and conjugated structure of graphite were not defected. The cyclic voltammograms were recorded in an alkaline solution. The observed pristine graphite voltammogram is attributed to the oxidation of solvent via the following reaction:

$$2H_2O \rightarrow O_2 + 4H^+ + 4e^-$$

For EF-graphite, the potential peak is shifted to less positive values with a higher current which can be due to better oxidation of amino acid amine groups presented in EF-graphite. Based on CV curves, it is found that the edge functionalization of graphite with L-phenylalanine did not demolish the electrical conductivity of graphite and enhanced electron transfer capability compared to pristine graphite owing to the existence of EF-graphite amine groups.

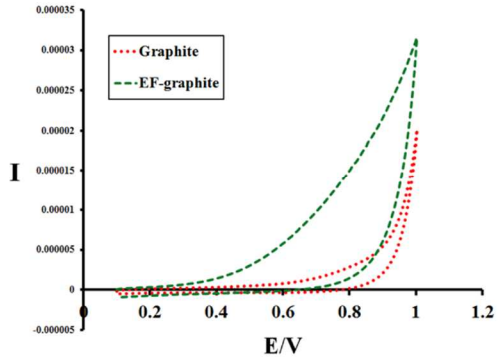

Fig. 9 Cyclic voltammogram of graphite and EF-graphite on the glassy carbon (GC) electrode.

Conclusions

Edge functionalization is one of the most appropriate ways to survive graphene-conjugated structure towards their applications in electronic devices. In conclusion, an effective preparation method was used in this study for the edge-selective functionalization of graphite by biocompatible L-phenylalanine amino acid in PPA/P_2O_5 medium. The covalent functionalization was verified by elemental analysis, FT-IR, XPS, and Raman spectroscopy. Based on TGA and XPS results, it is concluded that graphite is not oxidized during the edge-functionalization in PPA/P_2O_5 medium; and all of the characterization techniques revealed that the reaction exclusively occurs at the edge sites not on the basal plane. In addition, based on electrochemical study, the edge functionalization of graphite with L-phenylalanine did not eradicate the electrical conductivity of graphite; rather, it enhanced electron transfer capability compared to the pristine graphite.

Acknowledgements

We gratefully acknowledge the partial financial support from the Research Affairs Division Isfahan University of Technology (IUT), Isfahan. Further partial financial support of Iran Nanotechnology Initiative Council (INIC), National Elite Foundation (NEF) and Center of Excellency in Sensors and Green Chemistry (IUT) is also gratefully acknowledged.

Notes and references

[a] Organic Polymer Chemistry Research Laboratory, Department of Chemistry, Isfahan University of Technology, Isfahan, 84156-83111, I. R. Corresponding authors: Tel.: +98-31-33913249/+98-31-33913267; Fax: +98 31-33912350. E-mail addresses: abdolmaleki@cc.iut.ac.ir, amirabdolmaleki@yahoo.com/ mallak@cc.iut.ac.ir, mallak777@yahoo.com, mallakpour84@alumni.ufl.edu
[b] Nanotechnology and Advanced Materials Institute, Isfahan University of Technology, Isfahan, 84156-83111, I. R. Iran.
[c] Center of Excellence in Sensors and Green Chemistry, Department of Chemistry, Isfahan University of Technology, Isfahan, 84156-83111, I. R. Iran.

1. Y. H. Lu, W. Chen, Y. P. Feng and P. M. He, *The Journal of Physical Chemistry B*, 2008, **113**, 2-5.
2. L. Yan, Y. B. Zheng, F. Zhao, S. Li, X. Gao, B. Xu, P. S. Weiss and Y. Zhao, *Chem. Soc. Rev.*, 2012, **41**, 97-114.
3. C. Soldano, A. Mahmood and E. Dujardin, *Carbon*, 2010, **48**, 2127-2150.
4. K. I. Bolotin, K. J. Sikes, Z. Jiang, M. Klima, G. Fudenberg, J. Hone, P. Kim and H. L. Stormer, *Solid State Commun.*, 2008, **146**, 351-355.
5. Y. Zhu, S. Murali, W. Cai, X. Li, J. W. Suk, J. R. Potts and R. S. Ruoff, *Adv. Mater.*, 2010, **22**, 3906-3924.
6. J. Wu, W. Pisula and K. Müllen, *Chem. Rev.*, 2007, **107**, 718-747.
7. M. J. Allen, V. C. Tung and R. B. Kaner, *Chem. Rev.*, 2009, **110**, 132-145.
8. J. H. Jung, D. S. Cheon, F. Liu, K. B. Lee and T. S. Seo, *Angew. Chem. Int. Ed.*, 2010, **49**, 5708-5711.
9. S. J. Chae, F. Güneş, K. K. Kim, E. S. Kim, G. H. Han, S. M. Kim, H.-J. Shin, S.-M. Yoon, J.-Y. Choi, M. H. Park, C. W. Yang, D. Pribat and Y. H. Lee, *Adv. Mater.*, 2009, **21**, 2328-2333.
10. T. Kuila, S. Bose, A. K. Mishra, P. Khanra, N. H. Kim and J. H. Lee, *Prog. Mater Sci.*, 2012, **57**, 1061-1105.
11. Z. Mo, H. Gou, J. He, P. Yang, C. Feng and R. Guo, *Appl. Surf. Sci.*, 2012, **258**, 8623– 8628.
12. S. Mallakpour, A. Abdolmaleki and S. Borandeh, *Appl. Surf. Sci.*, 2014, **307**, 533-542.
13. S. P. Economopoulos and N. Tagmatarchis, *Chemistry – A European Journal*, 2013, **19**, 12930-12936.
14. C. K. Chua and M. Pumera, *Chem. Soc. Rev.*, 2013, **42**, 3222-3233.

15. M. Quintana, E. Vazquez and M. Prato, *Acc. Chem. Res.*, 2012, **46**, 138-148.
16. C. Shan, H. Yang, D. Han, Q. Zhang, A. Ivaska and L. Niu, *Langmuir*, 2009, **25**, 12030–12033.
17. M. Cano, U. Khan, T. Sainsbury, A. O'Neill, Z. Wang, I. T. McGovern, W. K. Maser, A. M. Benito and J. N. Coleman, *Carbon*, 2013, **52**, 363-371.
18. L. Gao, H. Zhang and H. Cui, *Biosens. Bioelectron.*, 2014, **57**, 65-70.
19. W. Cai, R. D. Piner, F. J. Stadermann, S. Park, M. A. Shaibat, Y. Ishii, D. Yang, A. Velamakanni, S. J. An, M. Stoller, J. An, D. Chen and R. S. Ruoff, *Science*, 2008, **321**, 1815-1817.
20. A. Lerf, H. He, M. Forster and J. Klinowski, *The Journal of Physical Chemistry B*, 1998, **102**, 4477-4482.
21. H. He, J. Klinowski, M. Forster and A. Lerf, *Chem. Phys. Lett.*, 1998, **287**, 53-56.
22. H. He, T. Riedl, A. Lerf and J. Klinowski, *The Journal of Physical Chemistry*, 1996, **100**, 19954-19958.
23. T. S. Sreeprasad and V. Berry, *Small*, 2013, **9**, 341-350.
24. L. J. Cote, J. Kim, V. C. Tung, J. Luo, F. Kim and J. Huang, *Pure Appl. Chem.*, 2011, **83**, 95-110.
25. S. Park, J. An, J. R. Potts, A. Velamakanni, S. Murali and R. S. Ruoff, *Carbon*, 2011, **49**, 3019-3023.
26. W. Hou, B. Tang, L. Lu, J. Sun, J. Wang, C. Qin and L. Dai, *RSC Advances*, 2014, **4**, 4848-4855.
27. P. Khanra, T. Kuila, N. H. Kim, S. H. Bae, D.-s. Yu and J. H. Lee, *Chem. Eng. J.*, 2012, **183**, 526-533.
28. S. Pei and H.-M. Cheng, *Carbon*, 2012, **50**, 3210-3228.
29. M. J. Fernández-Merino, L. Guardia, J. I. Paredes, S. Villar-Rodil, P. Solís-Fernández, A. Martínez-Alonso and J. M. D. Tascón, *The Journal of Physical Chemistry C*, 2010, **114**, 6426-6432.
30. D. W. Chang, H. J. Choi, I. Y. Jeon and J. B. Baek, *Chemical Record*, 2013, **13**, 224-238.
31. E.-K. Choi, I.-Y. Jeon, S.-Y. Bae, H.-J. Lee, H. S. Shin, L. Dai and J.-B. Baek, *Chem. Commun.*, 2010, **46**, 6320-6322.
32. I.-Y. Jeon, D. Yu, S.-Y. Bae, H.-J. Choi, D. W. Chang, L. Dai and J.-B. Baek, *Chem. Mater.*, 2011, **23**, 3987-3992.
33. I.-Y. Jeon, H.-J. Choi, S.-M. Jung, J.-M. Seo, M.-J. Kim, L. Dai and J.-B. Baek, *J. Am. Chem. Soc.*, 2012, **135**, 1386-1393.
34. K.-S. Kim, I.-Y. Jeon, S.-N. Ahn, Y.-D. Kwon and J.-B. Baek, *J. Mater. Chem.*, 2011, **21**, 7337-7342.
35. J. Y. Baek, I.-Y. Jeon and J.-B. Baek, *Journal of Materials Chemistry A*, 2014, **2**, 8690-8695.
36. I.-Y. Jeon, Y.-R. Shin, G.-J. Sohn, H.-J. Choi, S.-Y. Bae, J. Mahmood, S.-M. Jung, J.-M. Seo, M.-J. Kim, D. W. Chang, L. Dai and J.-B. Baek, *Proc. Natl. Acad. Sci. U.S.A.*, 2012, **109**, 5588–5593.
37. S.-Y. Bae, I.-Y. Jeon, J. Yang, N. Park, H. S. Shin, S. Park, R. S. Ruoff, L. Dai and J.-B. Baek, *ACS Nano*, 2011, **5**, 4974-4980.
38. E.-K. Choi, I.-Y. Jeon, S.-J. Oh and J.-B. Baek, *J. Mater. Chem.*, 2010, **20**, 10936-10942.
39. R. Nielsen, P. Kingshott, T. Uyar, J. Hacaloglu and K. L. Larsen, *Surf. Interface Anal.*, 2011, **43**, 884-892.
40. J.-Y. Wang, S.-Y. Yang, Y.-L. Huang, H.-W. Tien, W.-K. Chin and C.-C. M. Ma, *J. Mater. Chem.*, 2011, **21**, 13569-13575.
41. C. Xu, Y. Cao, R. Kumar, X. Wu, X. Wang and K. Scott, *J. Mater. Chem.*, 2011, **21**, 11359-11364.
42. M. S. Ahmed, H. S. Han and S. Jeon, *Carbon*, 2013, **61**, 164-172.